

DOI: ADD DOINUMBER HERE

A BGK model for high temperature rarefied hypersonic flows

C Baranger*[†], Y. Dauvois*, G. Marois*, J. Mathé*, J. Mathiaud*, L. Mieussens*

*CEA-CESTA 15 avenue des Sablières CS 60001 33116 Le Barp Cedex France

* Institut de Mathématiques de Bordeaux (UMR 5251), Univ. Bordeaux, 351, cours de la libération, 33405 Talence France

celine.baranger@cea.fr · yann.dauvois@cea.fr · gentien.marois@cea.fr · jordane.mathe@cea.fr
julien.mathiaud@cea.fr · Luc.Mieussens@math.u-bordeaux.fr

[†]Corresponding author

Abstract

To compute parietal flux and aerodynamic coefficients of space shuttles, one has to simulate precisely hypersonic flows around them. In the upper layers of the atmosphere, the air is in a rarefied state and described by Boltzmann-like equation. We develop a BGK model for real gas (polyatomic, with small Prandtl number) to simulate such flows. In such hypersonic flows, high temperature gases show complex phenomena like excitation of rotational and vibrational energy modes, and even chemical reactions. For flows in the continuous regime, simulation codes use analytic or tabulated constitutive laws for pressure and temperature. In this paper, we propose a BGK model which is consistent with any arbitrary constitutive laws, and which is designed to make high temperature gas flow simulations in the rarefied regime. This model is also consistent with the corresponding Navier-Stokes model for continuous regime in the small Knudsen number limit. By standard reduced technique, we obtain a kinetic model for high temperature polyatomic gases with a computational cost close to that of a simple monoatomic gas. Our approach will be illustrated by a numerical comparison with a compressible Navier-Stokes solver with rotational and vibrational non-equilibrium.

1. Introduction

During re-entry of space shuttle, various kind of atmospheric layers are encountered at high speed. To develop such shuttles, one has to compute parietal flux and aerodynamic coefficients on these objects, which implies to simulate precisely air flows around them. In the upper layers of the atmosphere, the air is in a rarefied state, the mean free path of the particles of air is not so small as compared to the size of the shuttle. In such a rarefied regime, the Knudsen number which is the ratio between the mean free path λ and a characteristic length L ($Kn = \frac{\lambda}{L}$) is larger than 0.01, and is used to discriminate rarefied regime from continuous regime (at low altitude) and also from the molecular regime (very high altitude). In the continuous regime, the flow is described by the compressible Navier-Stokes equations of Gas Dynamics. In the molecular regime, the Newton law is used to describe quantities at the boundary of the shuttle. In the rarefied regime, the Navier-Stokes equations are no longer valid and the use of the kinetic theory of gas *via* the Boltzmann equation is needed. The evolution of the molecules of the gas is then described by a mass density distribution in phase space, which is a solution of the Boltzmann equation. In the transitional regime (from rarefied to the beginning of continuous regime), this equation can be replaced by the simpler Bhatnagar-Gross-Krook (BGK) model: the complex collision term of the Boltzmann equation is replaced by a relaxation toward the equilibrium. This model is simpler than the Boltzmann equation but keeps the same conservation properties. However, it relies on a simple gas model (monoatomic for example).

The most popular numerical method to simulate rarefied flows is the Direct Simulation Monte Carlo method (DSMC).⁸ However, it is well known that this method is very expensive in transitional regimes, in particular for flows in the range of altitude we are interested in here. In contrast, deterministic methods (based on a numerical discretization of the stationary kinetic model) can be more efficient in transitional regimes. In our team at the CEA (French Atomic Energy Agency), we developed several years ago a deterministic code to make 2D plane and axisymmetric simulations of rarefied flows based on the BGK model. This code has been extended to 3D computations, for polyatomic gases. The BGK model is approximate with a discrete velocity method and a deterministic solver. A finite volume scheme is used to achieve stationary computations (see^{3-5,12,13}).

SIMULATION OF HYPERSONIC RAREFIED FLOWS

Due to the physical model (polyatomic gases), the space discretization (block structured mesh), and the parallelisation (space domain decomposition with MPI and inner parallelisation with OpenMP), this code is rather different from the other existing 3D codes recently presented in the literature for the same kind of problems (the 3D code of Titarev¹⁴ for example). In order to be able to achieve realistic simulations (3D configurations with Mach number up to 20), the method to discretize the velocity space has to be modified in order to decrease CPU time and memory storage requirements. We presented recently^{4,5} our new strategy to reduce the cost of computation: the locally refined discrete velocity grids. The use of this AMR (Adaptative Mesh Refinement) velocity grid was a significant improvement in term of computational cost. With such strategy, realistic computations (3D and high Mach number) are now available. In order to be able to treat realistic configurations, the BGK-model was updated. It is well known that the BGK equation leads to a Prandtl number (ratio between viscous effect to thermal effect) equal to 1. We presented in⁷ the ES-BGK model (described in²) which enables realistic Prandtl number and the extension of this model to polyatomic gases.

We will present in this paper the extension of the BGK model in order to take into account the high temperature effect on gases: in hypersonic flows, temperature around the wall of the shuttle can be very high, and complex phenomena will appear, like rotational and vibrational energy modes of the molecules of the polyatomic gases (for example, for air, N_2 and O_2). Chemical reactions as also to be consider. For flows in the continuous regime, simulation codes use analytic or tabulated constitutive laws for pressure and temperature. In this paper, we propose a BGK model which is consistent with any arbitrary constitutive laws, and which is designed to make high temperature gas flow simulations in the rarefied regime. This model is also consistent with the corresponding Navier-Stokes model for continuous regime in the small Knudsen number limit. By standard reduced technique, we obtain a kinetic model for high temperature polyatomic gases with a computational cost close to that of a simple monoatomic gas. Our approach will be illustrated by a numerical comparison with a compressible Navier-Stokes solver with rotational and vibrational non-equilibrium.

2. Kinetic Model for hypersonic rarefied flows

In the rarefied regime, the molecules of the gas in the flow are described by the distribution function $f \equiv f(t, \mathbf{x}, \mathbf{v})$ depending on time t , position $\mathbf{x} \in \mathbb{R}^3$ and speed $\mathbf{v} \in \mathbb{R}^3$. This function is the solution of the Boltzmann equation.

2.1 BGK model

As we are interested in the transitional regime, where the Knudsen number is between 0.01 to 1, we use here the Bathnagar, Gross, and Krook model (BGK). The collision term of the Boltzmann equation is replaced by a relaxation toward equilibrium:

$$\frac{\partial f}{\partial t} + \mathbf{v} \cdot \nabla_{\mathbf{x}} f = \frac{1}{\tau} (\mathcal{M}(f) - f) \quad (1)$$

The first part of the equation solves the moving state of the particles, and the right hand side of the equation is the relaxation toward the equilibrium $\mathcal{M}(f)$ called a Maxwellian:

$$\mathcal{M}(f) = \frac{\rho}{(2\pi RT)^{3/2}} e^{-\frac{|\mathbf{v}-\mathbf{u}|^2}{2RT}} = \mathcal{M}(\rho, \mathbf{u}, T) \quad (2)$$

Here, the macroscopic quantities ρ , \mathbf{u} and T , depending on time and space, are related to the first three moments of the distribution function f . The relaxation rate $\tau = \tau(t, \mathbf{x})$ depends on macroscopic quantities of the flow like pressure and viscosity.

This equation is supplemented by boundary conditions. Far from the boundary of the flying object, the distribution function is determined with the characteristic of the atmosphere (pressure and density), and with the velocity of the object (we compute in the relative referential). At the boundary of the object, several conditions can be applied: diffusive reflection of the particles on the wall, specular reflection or mixed condition with an accommodation coefficient. This coefficient is supposed to be related to the state of the surface of the body. It is still a challenge to determine precisely the value of this coefficient.

The BGK model preserves the mass, momentum and kinetic energy of the particles and the entropy dissipation (H-theorem). By integrating the distribution function with respect to the velocity \mathbf{v} , we define the macroscopic quantities ρ , \mathbf{u} , \mathbf{T} :

$$\begin{pmatrix} \rho \\ \rho \mathbf{u} \\ \frac{3}{2} \rho RT \end{pmatrix} = \int_{\mathbf{v}} \begin{pmatrix} f(t, \mathbf{x}, \mathbf{v}) \\ \mathbf{v} f(t, \mathbf{x}, \mathbf{v}) \\ \frac{1}{2} |\mathbf{v} - \mathbf{u}|^2 f(t, \mathbf{x}, \mathbf{v}) \end{pmatrix} d\mathbf{v} \quad (3)$$

When the Knudsen number tends to 0 (i.e. the continuous regime), the macroscopic quantities (ρ , $\rho \mathbf{u}$, ρT) are solution of the asymptotic limit of the BGK model: the Navier-Stokes equations. We are then able to compare the solutions of the two systems, the macroscopic quantities computed from the rarefied solution of the BGK model and the solution of the Navier-Stokes equations.

We plot on the figure 1 the pressure, temperature and Mach number for a flow around a sphere of 0.1 m diameter. The flow is at Mach 5, pressure 22.14 Pa and density $3.14 \cdot 10^{-4} \text{ kg.m}^{-3}$ (approximately 60 km altitude). The Knudsen number is then of order $2 \cdot 10^{-3}$, and is small enough so that the continuous and rarefied solutions are close. On the figure 1, we plot the pressure, temperature and Mach number for the Navier-Stokes (bottom) and BGK solution (top). The macroscopic quantities are then very close. We have to mention here that the Navier-Stokes solution was obtained with the fixed Pr parameter equal to 1 and that the flow is consider to be a perfect gas, with classical viscosity for air (see subsection 2.2).

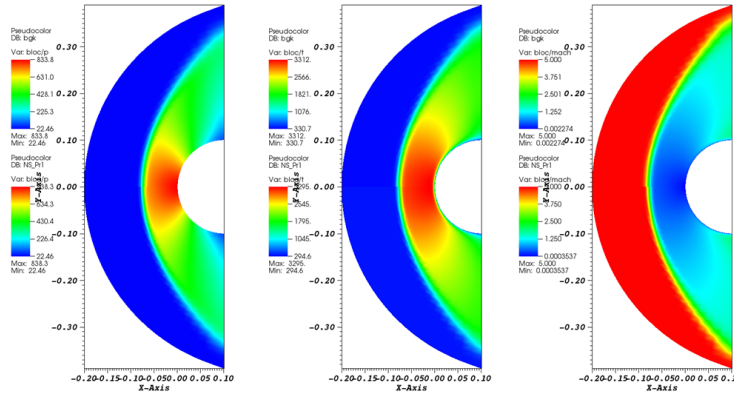


Figure 1: The pressure, temperature and Mach number between BGK solution (top) and Navier-Stokes solution (bottom) for a flow at Mach 5 and Knudsen $2 \cdot 10^{-3}$

2.2 BGK-like models to describe atmospheric flow

To describe the air surrounding space shuttle during reentry, the BGK model has to be adapted to deal with real flow. The relaxation rate obtained by a Chapman-Enskog expansion from the Boltzmann model, is equal to:⁸

$$\tau = \frac{\mu}{P} = \frac{1}{P} \mu_{ref} \left(\frac{T}{T_{ref}} \right)^{\omega}, \quad (4)$$

where $\omega = 0.77$, $T_{ref} = 273K$, $\mu_{ref} = 1.719 \cdot 10^{-5} \text{ N.s.m}^{-2}$.

The gas in earth atmosphere is air which is composed by diatomic molecules (N_2 and O_2). The BGK model described above is dedicated to the description of monoatomic molecules (no additional parameters to deal with internal energy of the molecules). The extension⁹ of this model for polyatomic molecules has been made. The internal energy is an additional variable of the distribution function, and by the use of the reduced distribution technique, a system of two BGK equations is obtained.

The main drawback of the BGK model is that the viscous and thermal effects are not independent, so that realistic values of the transport coefficients (Prandtl number, second viscosity) are not achievable. The BGK model describe for example flow with Prandtl number equal to 1. But, air flows have Prandtl number around 0.72. The heat flux at the boundary is then underestimated with the classical BGK model. The ES-BGK model presented in (^{2,7,10}) gives the correct transport coefficients and Prandtl number.

2.3 ES-BGK model for real Prandtl number and perfect monoatomic gas

The idea of the Ellipsoidal Statistical model is to replace the Maxwellian function \mathcal{M} by a Gaussian function \mathcal{G} , and the temperature, by a tensor of temperature \mathcal{T} .

SIMULATION OF HYPERSONIC RAREFIED FLOWS

$$\frac{\partial f}{\partial t} + \mathbf{v} \cdot \nabla_{\mathbf{x}} f = \frac{1}{\tau} (\mathcal{G}(\rho, \mathbf{u}, \mathcal{T}) - f) \quad (5)$$

with $\mathcal{G}(\rho, \mathbf{u}, \mathcal{T}) = \frac{\rho}{\sqrt{\det(2\pi\mathcal{T})}} e^{-\frac{(\mathbf{v}-\mathbf{u})^T \mathcal{T}^{-1} (\mathbf{v}-\mathbf{u})}{2}}$ and

$$\tau = \frac{\mu}{Pr \rho R T}.$$

The tensor of temperature is defined by $\mathcal{T} = (1 - \nu)RT\mathbf{I}d + \nu\Theta$, where $\Theta = \frac{1}{\rho} \int (\mathbf{v} - \mathbf{u}) \otimes (\mathbf{v} - \mathbf{u}) f$ and the macroscopic temperature still determined by $T = \frac{1}{3\rho R} \int_{\mathbf{v}} |\mathbf{v} - \mathbf{u}|^2 f d\mathbf{v}$.

The Prandtl number is obtain by a Chapmann-Enskog expansion

$$Pr = \frac{1}{1 - \nu} \quad (6)$$

Then, for a monoatomic gas with $\nu = -0.5$, we recover the classical value $Pr = \frac{2}{3}$. The classical BGK model is included in the ES-BGK model as it corresponds to the value $\nu = 0$.

On figure 2.3, we present the result of the ES-BGK model with $Pr = 2/3$ and compare it to the previous solution of BGK ($Pr = 1$) and with Navier-Stokes ($Pr = 1$ and $2/3$). We have good agreement between the solutions with same Prandtl number. This ensures the validity of the ES-BGK model for monoatomic gases.

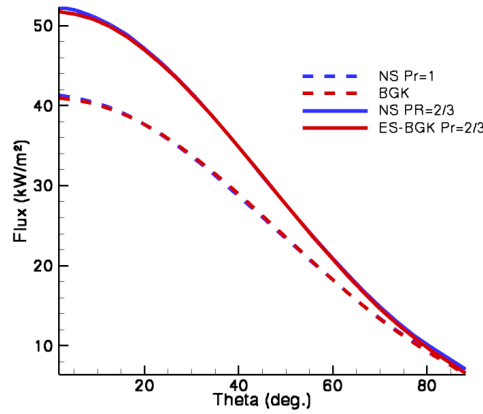


Figure 2: Comparison between Navier-Stokes ($Pr = 1$ and $2/3$), BGK and ES-BGK

2.4 ES-BGK model for perfect polyatomic gases (Air, Nitrogen, etc...)

When we are interested in simulate reentry in atmosphere composed by air, the model of ES-BGK presented previously is not suitable to describe polyatomic gas. An extension of the BGK model was proposed⁹ by the use of the reduction technique and we extend this model in order to take into account a non equal to 1 Prandtl number. The idea of the model for polyatomic gas is the following: a new variable has to be added in the definition of the density function $f \equiv f(t, \mathbf{x}, \mathbf{v}, I)$ where I is the internal energy. When collisions occur between polyatomic molecules, the total energy (kinetic and internal energies) is conserved and not only the kinetic energy : a part of the kinetic energy will be transformed into internal energy (rotational or vibrational energy). The problem of this method is that it adds a new variable in the phase space and that its numerical solving is much more expensive. The reduced distribution technique consists in solving only the first two moments of f in the I variable: $\tilde{f} = \int_0^{+\infty} f(t, \mathbf{x}, \mathbf{v}, I) dI$ and $\tilde{g} = \int_0^{+\infty} I^{2/\delta} f(t, \mathbf{x}, \mathbf{v}, I) dI$. δ is the degree of freedom of the gas ($\delta = 2$ for diatomic gases). These two functions are solutions of the closed system of BGK equations:

$$\begin{aligned} \frac{\partial \tilde{f}}{\partial t} + \mathbf{v} \cdot \nabla_{\mathbf{x}} \tilde{f} &= \frac{1}{\tau} (\mathcal{M}(\rho, \mathbf{u}, T) - \tilde{f}) \\ \frac{\partial \tilde{g}}{\partial t} + \mathbf{v} \cdot \nabla_{\mathbf{x}} \tilde{g} &= \frac{1}{\tau} \left(\frac{\delta RT}{2} \mathcal{M}(\rho, \mathbf{u}, T) - \tilde{g} \right) \end{aligned}$$

By now, we will denote \tilde{f} by f and \tilde{g} by g .

Like in the ES-BGK model for monoatomic gas, a correct Prandtl number can be obtained by replacing the Maxwellian function $\mathcal{M}(\rho, \mathbf{u}, T)$ by an anisotropic Gaussian function $\mathcal{G}(\rho, \mathbf{u}, \mathcal{T})$:

$$\begin{aligned}\frac{\partial f}{\partial t} + \mathbf{v} \cdot \nabla_{\mathbf{x}} f &= \frac{1}{\tau} (\mathcal{G}(\rho, \mathbf{u}, \mathcal{T}) - f) \\ \frac{\partial g}{\partial t} + \mathbf{v} \cdot \nabla_{\mathbf{x}} g &= \frac{1}{\tau} \left(\frac{\delta RT_{rel}}{2} \mathcal{G}(\rho, \mathbf{u}, \mathcal{T}) - g \right)\end{aligned}$$

with $T_{rel} = \theta T + (1 - \theta)T_{int}$ and $T_{tr} = \frac{1}{3\rho R} \int_{\mathbf{v}} |\mathbf{v} - \mathbf{u}|^2 f d\mathbf{v}$ $T_{int} = \frac{1}{\delta\rho R} \int_{\mathbf{v}} g d\mathbf{v}$, $T = \frac{3}{3+\delta}T_{tr} + \frac{\delta}{3+\delta}T_{int}$, and the tensor of temperature \mathcal{T} depends on two parameters (θ, ν) .

$$\mathcal{T} = (1 - \theta) \left((1 - \nu)RT_{tr}\mathbf{Id} + \nu\Theta \right) + \theta RT\mathbf{Id}$$

Then, the Prandtl number is

$$Pr = \frac{1}{1 - (1 - \theta)\nu}$$

With $\nu = -0.5$, $\theta = \frac{1}{5}$, we recover the Prandtl number for perfect polyatomic gas : $Pr = \frac{5}{7}$. For air, the Prandtl number is estimated at $Pr = 0.72$. The exchange of energy between translational and internal modes is driven by the parameter θ , which is adjusted by the formula of Lordi and Park⁸ : $\theta = \frac{1}{Z_{rot}(T)}$.

3. High temperature gases

In the flow around the shuttle, temperature can be up to 1000K. At this level, new phenomena appear (vibration, chemical reactions, ionization). For instance, for dioxygen, at 800K, the molecules begin to vibrate, and chemical reactions occur for much larger temperatures (for instance, dissociation of O_2 into O starts at 2500K).

In this section, we will present some of these effects (vibrations and chemical reactions) and how it can be taken into accounts in terms of equation of state (EOS) and number of internal degrees of freedom.

3.1 Vibrations

Of course, the definition of the specific internal energy must account for vibrational energy. A possible way to do so is to increase the number of internal degrees of freedom δ , that now accounts for rotational and vibrational modes. However, a result of quantum mechanics implies that this number of degrees of freedom is not an integer anymore, and that it is even not a constant (it is temperature dependent), see the examples below. Vibrating gases have other properties that make them quite different to what is described by the standard kinetic theory of monoatomic gases. For instance, the specific heat at constant pressure c_p becomes temperature dependent. However, vibrating gases can still be considered as perfect gases, so that the perfect EOS $p = \rho RT$ still holds (in fact, such gases are called thermally perfect gases, see¹).

Now we give two examples of gases with vibrational excitation, and we explain how their number of internal degrees of freedom is defined.

3.1.1 Example 1: dioxygen

At equilibrium, translational e_{tr} and rotational e_{rot} specific energies can be defined by

$$e_{tr} = \frac{3}{2}RT \quad \text{and} \quad e_{rot} = RT.$$

This shows that a molecule of dioxygen has 3 degrees of freedom for translation, and 2 for rotation. By using quantum mechanics,¹ vibrational specific energy e_{vib} is found to be

$$e_{vib} = \frac{T_{O_2}^{vib}/T}{\exp(T_{O_2}^{vib}/T) - 1} RT,$$

where $T_{O_2}^{vib} = 2256K$ is a reference temperature.

SIMULATION OF HYPERSONIC RAREFIED FLOWS

The number of “internal” degrees of freedom δ , related to rotation and vibration modes only, is defined such that the total specific internal energy e is

$$e = e_{tr} + e_{rot} + e_{vib} = \frac{3 + \delta}{2} RT.$$

By combining this relation with the relations above, we find that δ is actually temperature dependent, and defined by

$$\delta(T) = 2 + 2 \frac{T_{O_2}^{vib}/T}{\exp(T_{O_2}^{vib}/T) - 1}.$$

Accordingly, the specific heat at constant pressure c_p , which is defined by $dh = c_p dT$, where the enthalpy is $h = e + \frac{p}{\rho}$, can be computed as follows. Since $p = \rho RT$, we find $h = \frac{5+\delta(T)}{2} RT$, and hence the enthalpy depends on T only, through a nonlinear relation. This means that $c_p = h'(T)$ is not a constant anymore, while we have $c_p = \frac{5+\delta}{2} R$ without vibrations. Finally, note that the relation that defines the temperature T through the internal specific energy $e = \frac{3+\delta(T)}{2} RT$ now is nonlinear (it has to be inverted numerically to find T).

3.1.2 Example 2: air

The air at moderately high temperatures ($T < 2500K$) is a non-reacting mixture of nitrogen N_2 and dioxygen O_2 , whose mass concentrations are approximately $c_{N_2} = 75\%$ and $c_{O_2} = 25\%$. These two species are perfect gases with their own gas constants R_{N_2} and R_{O_2} . The gas constant R of the mixture can be defined by $R = c_{N_2} R_{N_2} + c_{O_2} R_{O_2}$ (see¹).

The specific internal energy is defined by $e = c_{O_2} e_{O_2} + c_{N_2} e_{N_2}$. The energy of each species can be computed like in our first example (see section 3.1.1), and we find:

$$e_{N_2} = \frac{3 + \delta_{N_2}(T)}{2} R_{N_2} T \quad \text{and} \quad e_{O_2} = \frac{3 + \delta_{O_2}(T)}{2} R_{O_2} T,$$

where the number of internal degrees of freedom of each species are

$$\delta_{N_2}(T) = 2 + 2 \frac{T_{N_2}^{vib}/T}{\exp(T_{N_2}^{vib}/T) - 1} \quad \text{and} \quad \delta_{O_2}(T) = 2 + 2 \frac{T_{O_2}^{vib}/T}{\exp(T_{O_2}^{vib}/T) - 1}, \quad (7)$$

with $T_{N_2}^{vib} = 3373K$ and $T_{O_2}^{vib} = 2256K$. Then the specific internal energy of the mixture is

$$\begin{aligned} e &= c_{O_2} \frac{3 + \delta_{O_2}(T)}{2} R_{O_2} T + c_{N_2} \frac{3 + \delta_{N_2}(T)}{2} R_{N_2} T \\ &= \frac{3}{2} RT + \frac{1}{2} (c_{O_2} \delta_{O_2}(T) R_{O_2} + c_{N_2} \delta_{N_2}(T) R_{N_2}) T \\ &= \frac{3 + \delta(T)}{2} RT \end{aligned}$$

with the number of internal degrees of freedom given by

$$\begin{aligned} \delta(T) &= \frac{c_{O_2} \delta_{O_2} R_{O_2} + c_{N_2} \delta_{N_2}(T) R_{N_2}}{R} \\ &= 2 + \frac{2}{R} \left(c_{O_2} R_{O_2} \frac{T_{O_2}^{vib}/T}{\exp(T_{O_2}^{vib}/T) - 1} + c_{N_2} R_{N_2} \frac{T_{N_2}^{vib}/T}{\exp(T_{N_2}^{vib}/T) - 1} \right). \end{aligned} \quad (8)$$

We show in figure 3 the number of internal degrees of freedom for each species and for the whole mixture. For all gases, δ is equal to 2 below 500K, which means that only the rotational modes are excited: each species is a diatomic gas with 2 degrees of freedom of rotation, and the mixture behaves like a diatomic gas too. Then the number of degrees of freedom increases with the temperature, and is greater than 2.5 for $T = 3000K$. At this temperature, the number of degrees of freedom for vibrations is 0.7. Note that in addition to this graphical analysis, it can be analytically proved that all the δ computed here are increasing functions of T .

3.2 Chemical reactions

When chemical reactions have to be taken into account (for the air, this starts at 2500K), the perfect gas EOS still holds for each species, but the EOS for the reacting mixture is less simple. To avoid the numerical solving of the Navier-Stokes equations for all the species, in the case of an equilibrium chemically reacting gas, it is convenient to use

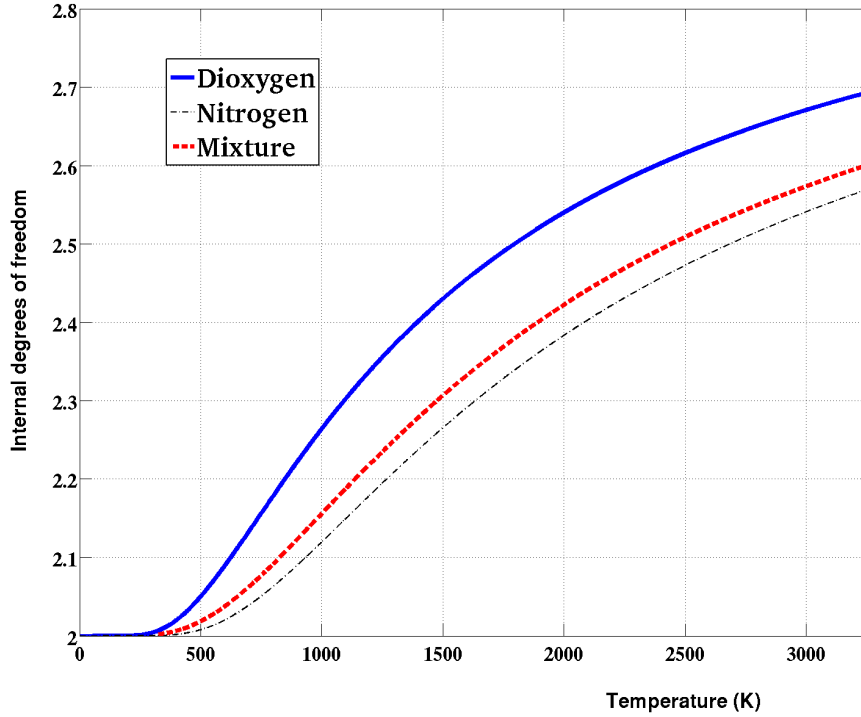


Figure 3: Internal degrees of freedom as a function of the temperature

instead a Navier-Stokes model for the mixture (considered as a single species), for which tabulated EOS $p = p(\rho, e)$ and even a tabulated temperature law $T = T(\rho, e)$ are used (see,¹ chapter 11).

More precisely, it can be shown that for a mixture of thermally perfect gases in chemical equilibrium, two state variables, like ρ and e , are sufficient to uniquely define the chemical composition of the mixture. Let us precise what this means, with notations that will be useful in the paper.

For every species of the mixture, numbered with index i :

- its concentration c_i depends on ρ and e only: $c_i = c_i(\rho, e)$;
- its pressure p_i satisfies the usual perfect gas law: $p_i = \rho_i R_i T$, where R_i is the gas constant of the species and $\rho_i = c_i(\rho, e)\rho$, so that $p_i = p_i(\rho, e)$;
- its specific energy e_i and enthalpy h_i depend on T only: $e_i = e_i(T)$ and $h_i = h_i(T)$, where $e_i(T) = \frac{3+\delta_i(T)}{2} R_i T + e_i^{f,0}$, with $e_i^{f,0}$ is the energy of formation of the i th molecule and $\delta_i(T)$ is the number of activated internal degrees of freedom of the molecule that might depend on the temperature, see the previous sections.

For compressible Navier-Stokes equations for an equilibrium chemically reacting mixture, these quantities are not necessary. Instead, it is sufficient to define (with analytic formulas or tables):

- the total pressure $p = \sum_i p_i(\rho, e)$ so that $p = p(\rho, e) = \rho R(\rho, e) T$, with $R(\rho, e) = \sum_i c_i(\rho, e) R_i$;
- the temperature T , though the relation $e = \sum_i c_i(\rho, e) e_i(T)$, so that $T = T(\rho, e)$;
- the total specific enthalpy $h = \sum_i c_i h_i$, so that $h = h(\rho, e) = e + \frac{p(\rho, e)}{\rho}$.

We refer to¹ for details on this subject.

4. BGK models for high temperature gases

4.1 A BGK model for arbitrary constitutive laws

In this section, we now want to extend the polyatomic ES-BGK model (7) so as to be consistent with arbitrary constitutive laws $p = p(\rho, e)$ and $T = T(\rho, e)$ that can be used for an equilibrium chemically reacting gas (see section 3.2). In this paper, we present only the case of a gas with Prandtl equal to 1, the ES version will be present in a future work.

SIMULATION OF HYPERSONIC RAREFIED FLOWS

The idea is here to modify the Maxwellian (2) so as to satisfy some constraints derived from the asymptotic fluid limits.

In the Euler limit, F converges towards its own local Maxwellian $M[F]$, and the dynamical pressure must be equal to the equilibrium kinetic pressure, that is to say

$$p(\rho, e) = \langle \langle |v - u|^2 M[F] \rangle \rangle.$$

Moreover, the internal energy must be equal to its equilibrium value, which gives:

$$\rho e = \langle \langle \left(\frac{1}{2} |v - u|^2 + \varepsilon \right) M[F] \rangle \rangle.$$

Using definition (2), we compute the two previous integrals to find the constraints

$$p(\rho, e) = \rho RT \quad \text{and} \quad \rho e = \frac{3 + \delta}{2} \rho RT.$$

These relations are satisfied if the product (gas constant \times temperature) used in the Maxwellian (2) is defined by $RT = p(\rho, e)/\rho$, which will be denoted by $\theta(\rho, e)$ in the following, and if δ is defined by $\delta(\rho, e) = \frac{2e}{p(\rho, e)/\rho} - 3$.

Moreover, the temperature $T(\rho, e)$ is taken into account through the relaxation time and the viscosity: relation (4) gives $\tau(\rho, e) = \mu(T(\rho, e))/p(\rho, e)$.

Finally, our BGK model is

$$\partial_t F + v \cdot \nabla_x F = \frac{1}{\tau(\rho, e)} (M[F] - F), \quad (9)$$

with

$$M[F] = \frac{\rho}{(2\pi\theta(\rho, e))^{\frac{3}{2}}} \exp\left(-\frac{|v - u|^2}{2\theta(\rho, e)}\right) \Lambda(\delta(\rho, e)) \left(\frac{\varepsilon}{\theta(\rho, e)}\right)^{\frac{\delta(\rho, e)}{2} - 1} \frac{1}{\theta(\rho, e)} \exp\left(-\frac{\varepsilon}{\theta(\rho, e)}\right), \quad (10)$$

where the macroscopic quantities are defined by

$$\rho(t, x) = \langle \langle F \rangle \rangle, \quad \rho u(t, x) = \langle \langle v F \rangle \rangle, \quad \rho e(t, x) = \langle \langle \left(\frac{1}{2} |v - u|^2 + \varepsilon \right) F \rangle \rangle, \quad (11)$$

the variable $\theta(\rho, e)$ is

$$\theta(\rho, e) = \frac{p(\rho, e)}{\rho}, \quad (12)$$

the number of internal degrees of freedom is

$$\delta(\rho, e) = \frac{2e}{p(\rho, e)/\rho} - 3. \quad (13)$$

and the relaxation time is

$$\tau(\rho, e) = \frac{\mu(T(\rho, e))}{p(\rho, e)}, \quad (14)$$

while, finally, $p(\rho, e)$, $T(\rho, e)$, and $\mu(T)$ are given by analytic formulas or numerical tables.

4.2 Compressible Navier-Stokes asymptotics

The moments of F , solution of the BGK model (9)–(14), satisfy the following Navier-Stokes equations, up to $O(\text{Kn}^2)$:

$$\begin{aligned} \partial_t \rho + \nabla \cdot \rho u &= 0, \\ \partial_t \rho u + \nabla \cdot (\rho u \otimes u) + \nabla p &= -\nabla \cdot \sigma, \\ \partial_t E + \nabla \cdot (E + p)u &= -\nabla \cdot q - \nabla \cdot (\sigma u), \end{aligned} \quad (15)$$

where Kn is the Knudsen number (defined below), E is the total energy density defined by $E = \frac{1}{2} \rho |u|^2 + \rho e$, and σ and q are the shear stress tensor and heat flux vector defined by

$$\begin{aligned} \sigma &= -\mu \left(\nabla u + (\nabla u)^T - C \nabla \cdot u Id \right), \\ q &= -\mu \nabla h, \end{aligned} \quad (16)$$

with $h = e + \frac{p(\rho, e)}{\rho}$ is the enthalpy, and $C = \frac{\rho^2}{p(\rho, e)} \partial_\rho \left(\frac{p(\rho, e)}{\rho} \right) + \partial_e \left(\frac{p(\rho, e)}{\rho} \right)$.

Note that this result is consistent with the Navier-Stokes equations obtained for non reacting gases. For instance, in case of a thermally perfect gas, i.e when the enthalpy depends only on the temperature (see¹), we find that the heat flux is $q = -\kappa \nabla T(\rho, e)$, where the heat transfer coefficient is $\kappa = \mu c_p$, with the heat capacity at constant pressure is $c_p = h'(T)$. In such case, the Prandtl number, defined by $\text{Pr} = \frac{\mu c_p}{\kappa}$, is 1, like in usual BGK models.

Moreover, this result gives a volume viscosity (also called second coefficient of viscosity or bulk viscosity) which is $\omega = \mu \left(\frac{2}{3} - C \right)$. In the case of a gas with a constant δ , like in a non vibrating gas, this gives $C = \frac{2}{3+\delta}$, and hence $\omega = \frac{2\delta}{3(\delta+3)}\mu$. For a monoatomic gas, $\delta = 0$, and we find the usual result $\omega = 0$.

This result can be proved by using the standard Chapman-Enskog expansion.

4.3 Reduced model

For computational reasons, it is interesting to reduce the complexity of model (9) by using the usual reduced distribution technique.¹¹ We define reduced distributions $f(t, x, v) = \int_0^{+\infty} F(t, x, v, \varepsilon) d\varepsilon$ and $g(t, x, v) = \int_0^{+\infty} \varepsilon F(t, x, v, \varepsilon) d\varepsilon$, and by integration of (9) w.r.t ε , we can easily obtain the following closed system of two BGK equations

$$\begin{aligned} \partial_t f + v \cdot \nabla_x f &= \frac{1}{\tau} (M[f, g] - f), \\ \partial_t g + v \cdot \nabla_x g &= \frac{1}{\tau} \left(\frac{\delta}{2} \frac{p}{\rho} M[f, g] - g \right), \end{aligned} \quad (17)$$

where $M[f, g]$ is the translational part of $M[F]$ defined by

$$M[f, g] = \frac{\rho}{(2\pi p/\rho)^{\frac{3}{2}}} \exp\left(-\frac{|v-u|^2}{2p/\rho}\right),$$

and the macroscopic quantities are defined by

$$\rho(t, x) = \int_{\mathbb{R}^3} f dv, \quad \rho u(t, x) = \int_{\mathbb{R}^3} v f dv, \quad \rho e(t, x) = \int_{\mathbb{R}^3} \left(\frac{1}{2} |v-u|^2 f + g \right) dv,$$

while δ and τ are still defined by (13) and (14). This reduced system is equivalent to (9), that is to say F and (f, g) have the same moments. Moreover, the compressible Navier-Stokes asymptotics obtained in section 4.2 can also be derived from this reduced system. Consequently, this is this system which is used in our numerical tests in the following section.

5. Numerical results

A numerical scheme for model (17) has been implemented in the code of CEA-CESTA. This code is a deterministic code based on the works presented in^{5,6,9} which solves the BGK equation in 3 dimensions of space and 3 dimensions in velocity with a second order finite volume scheme on structured meshes. It is remarkable that the original code (for non reacting gases, with no high temperature effects), presented in^{5,6} can be very easily adapted to this new model. Only a few modifications are necessary.

The goal of this section is to illustrate the capacity of our model to account for some high temperature gas effects. We only consider the case of a mixture of two vibrating, but non reacting, gases. A validation of our model for reacting gases will be given in a further work.

Our test is a 2D hypersonic plane flow of air—considered as a mixture of two vibrating gases, nitrogen and dioxygen, over a quarter of a cylinder which is supposed to be isothermal (see figure 1). Gas-solid wall interactions are modeled by the usual diffuse reflection. At the inlet, the flow is defined by the data given in table 1.

In this case, as the temperature T is a function of e , it can be written $T = T(\rho, e)$. Then, the perfect gas EOS $p = \rho RT(\rho, e)$ gives $p = p(\rho, e)$. Then, the number of internal degrees of freedom, given by (13) can be written $\delta(T) = 2 \frac{e}{RT} - 3$.

In this case, the vibrational energy is taken into account as described in section 3.1.2.

The flow conditions are such that molecules vibrate, but no chemical reactions are active (temperatures go up to 3000K whereas chemical reactions occur at 5000K at pressure $P = 1\text{atm}$): our thermodynamical approach is reasonable. Since the test case is dense enough (the Knudsen number is around 0.01) we can compare the new model with a Navier-Stokes code (a 2D finite volume code with structured meshes), in which are enforced the same viscosity and conductivity as in compressible Navier-Stokes asymptotics derived from the BGK model (see section 4.2). To validate the new model we have made four different simulations:

SIMULATION OF HYPERSONIC RAREFIED FLOWS

Mass concentration of N_2 (c_{N_2})	0.75
Mass concentration of O_2 (c_{O_2})	0.25
Mach number of the mixture	10
Velocity of the mixture	$2267m.s^{-1}$
Density of the mixture	$3.059 \times 10^{-4}kg.m^{-3}$
Pressure of the mixture	$11.22Pa$
Temperature of the mixture	$127.6K$
Temperature of the sphere	$293K$
Radius of the cylinder	$0.1m$

Table 1: Hypersonic flow around a cylinder: initial data

- a Navier-Stokes simulation without taking into account vibrations (called *NS1*),
- a Navier-Stokes simulation that takes into account vibrations (called *NS2*),
- a BGK simulation without taking into account vibrations (called *BGK1*),
- a BGK simulation that takes into account vibrations (called *BGK2*).

The first comparison is between *NS1* and *BGK1*, in order to show that the two model are consistent in this dense regimes, when there are no vibration energy. As it can be seen in figure 4, the results agree very well.

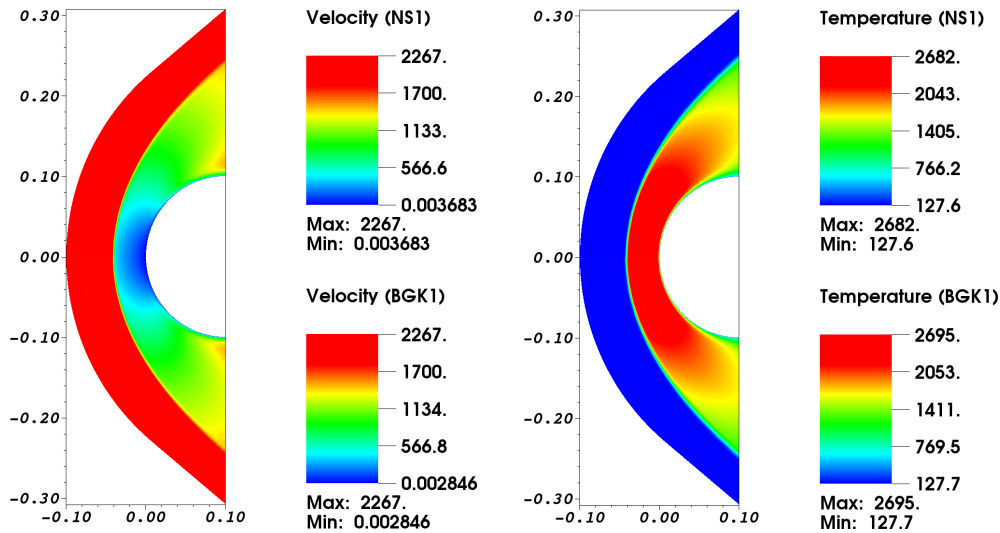


Figure 4: Non vibrating air: velocity and temperature fields (Top: NS1, bottom: BGK1)

The second comparison is between *NS2* and *BGK2* to show we still have a good agreement when vibrations are taken into account. This is what we observe in figure 5. One can also observe that, due to vibrations, the temperature decreased from $2682K$ to $2358K$ for Navier-Stokes and from $2695K$ to $2365K$ for BGK.

The last comparison is to show the influence of vibrational energy on the results. We compare *BGK1* and *BGK2*, and we observe that the shock is not at the same position. Since there is a transfer of energy from translational and rotational modes to vibrational modes, the maximum temperature is lower and the shock is slightly close to the cylinder with *BGK2* (see figure 6).

We clearly see this difference with the temperature profile along the stagnation line, see figure 7.

To conclude this section, it can be said that when Navier-Stokes and BGK are set with the same viscosity and Prandtl number, results agree very well: but of course for more realistic test cases when the Prandtl number is not equal to one, there will be a discrepancy in the results that might be corrected with an ES-BGK extension of our model. This will be presented in a further work.

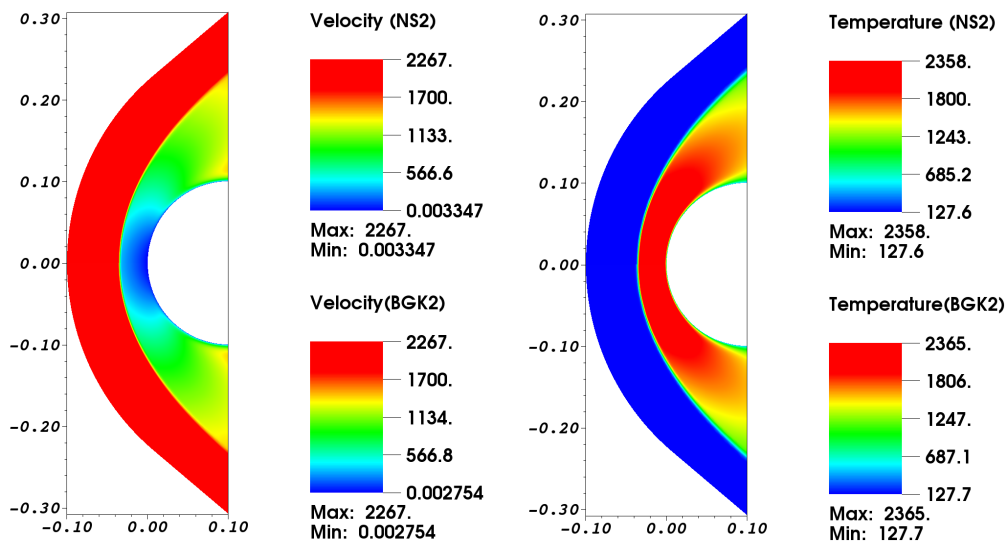


Figure 5: Vibrating air: velocity and temperature fields (Top: NS2, bottom: BGK2)

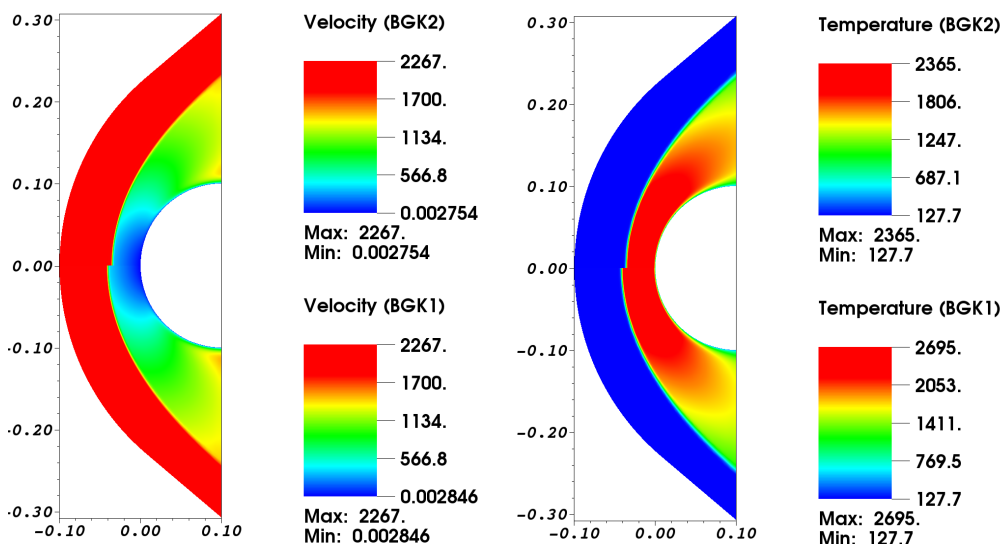


Figure 6: Vibrating and non-vibrating air: velocity field and temperature field (Top: BGK2, bottom: BGK1)

References

- [1] J. D. Anderson. *Hypersonic and high-temperature gas dynamics second edition*. American Institute of Aeronautics and Astronautics, 2006.
- [2] P. Andries, P. Le Tallec, J.-P. Perlat, and B. Perthame. The gaussian-bgk model of boltzmann equation with small prandtl number. *European Journal of Mechanics - B/Fluids*, 19(6):813 – 830, 2000.
- [3] K. Aoki, P. Degond, and L. Mieussens. Numerical simulations of rarefied gases in curved channels: thermal creep, circulating flow, and pumping effect. *Commun. Comput. Phys.*, 6:919–954, 2009.
- [4] C. Baranger, J. Claudel, N. Hérouard, and L. Mieussens. Locally refined discrete velocity grids for deterministic rarefied flow simulations. *AIP Conference Proceedings*, 1501(1):389–396, 2012.
- [5] C. Baranger, J. Claudel, N. Hérouard, and L. Mieussens. Locally refined discrete velocity grids for stationary rarefied flow simulations. *Journal of Computational Physics*, 257:572–593, 2014.

SIMULATION OF HYPERSONIC RAREFIED FLOWS

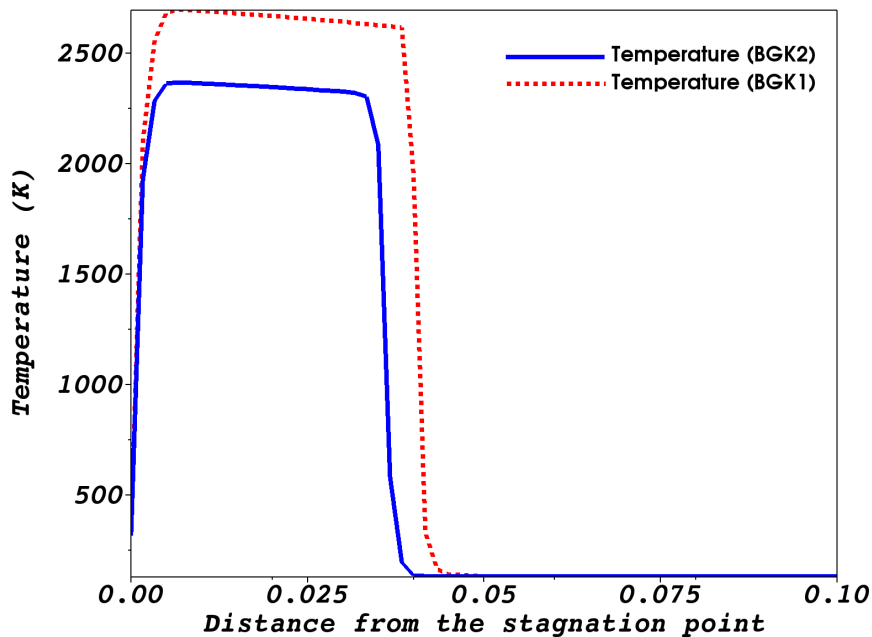


Figure 7: Vibrating and non-vibrating air: temperature profile along the stagnation line.

- [6] C. Baranger, N. Hérouard, J. Mathiaud, and L. Mieussens. Numerical boundary conditions in finite volume and discontinuous galerkin schemes for the simulation of rarefied flows along solid boundaries. *Mathematics and Computers in Simulation*, 159:136–153, 2019.
- [7] C. Baranger, N. Hérouard, J. Mathiaud, L. Mieussens, J.-F. Poustis, and al.. Modeling, numerical method and validation for the simulation of hypersonic rarefied gas flows. In *Proceedings of the 7th European Conference for Aeronautics and Space Sciences*, 2017.
- [8] G.A. Bird. *Molecular Gas Dynamics and the Direct Simulation of Gas Flows*. Oxford Science Publications, 1994.
- [9] B. Dubroca and L. Mieussens. A conservative and entropic discrete-velocity model for rarefied polyatomic gases. In *CEMRACS 1999 (Orsay)*, volume 10 of *ESAIM Proc.*, pages 127–139 (electronic). Soc. Math. Appl. Indust., Paris, 1999.
- [10] L. H. Holway. Kinetic theory of shock structure using an ellipsoidal distribution function. In New York Academic Press, editor, *Rarefied Gas Dynamics, Vol. 1 (Proc. Fourth Internat. Sympos. Univ. Toronto, 1964)*, pages 193–215, 1966.
- [11] A. B. Huang and D. L. Hartley. Nonlinear rarefied couette flow with heat transfer. *Phys. Fluids*, 11(6):1321, 1968.
- [12] L. Mieussens. Discrete Velocity Model and Implicit Scheme for the BGK Equation of Rarefied Gas Dynamics. *Math. Models and Meth. in Appl. Sci.*, 8(10):1121–1149, 2000.
- [13] L. Mieussens. Discrete-velocity models and numerical schemes for the Boltzmann-BGK equation in plane and axisymmetric geometries. *J. Comput. Phys.*, 162:429–466, 2000.
- [14] V. A. Titarev. Efficient deterministic modelling of three-dimensional rarefied gas flows. *Communications in Computational Physics*, 12(1):162–192, 2012.